*Acta Cryst.* (1996). B52, 59–65

# Neutron and X-ray Diffuse Scattering of Calcium-Stabilized Zirconia

TH. PROFFEN, R. B. NEDER AND F. FREY

*Institut für Kristallographie und Mineralogie, LMU München, Theresienstrasse 41, D-80333 München, Germany*

*(Received 5 May 1995; accepted 16 June 1995)*

## Abstract

The defect structure of calcium-stabilized zirconia (CSZ) is described in terms of a correlated distribution of microdomains within the cubic matrix of CSZ. The defect structure consists of two types of defects: microdomains based on a single oxygen vacancy with relaxed neighbouring ions and microdomains based on a pair of oxygen vacancies separated by $3^{1/2}/2a$ along <111>. The combined evaluation of neutron and X-ray data shows that the previously published structure of the single vacancy domain has to be modified: All cations next to the oxygen vacancy are most likely zirconium. This modified model leads to good agreement between observed and calculated neutron and X-ray diffraction patterns.

## 1. Introduction

The cubic phase of pure $ZrO_2$ is thermodynamically stable only at temperatures above 2643 K. This phase is stabilized by thermally induced oxygen vacancies (Rauh & Garg, 1980). By doping with oxides of various di- and trivalent metals (*e.g.* Ca, Mg and Y), the cubic phase can be stabilized at room temperature. The average structure is of the fluorite type, space group $Fm3m$, with zirconium on (0,0,0) and oxygen on $(\frac{1}{4},\frac{1}{4},\frac{1}{4})$. The stabilization is due to oxygen vacancies introduced by the dopant metal ion occupying the zirconium site (Subbarao, 1981). Ho (1982) suggests that the zirconium ions occupy seven-coordinated cation sites in the locally distorted fluorite-type structure.

Neder, Frey & Schulz (1990*b*) analysed the neutron diffuse scattering of CSZ doped with 15 mol% CaO by a model of a correlated distribution of microdomains* within the matrix of cubic zirconia. Neder, Frey & Schulz (1990*b*) introduced two types of microdomains, one based on a single oxygen vacancy with relaxed neighbouring ions and a second based on a pair of oxygen vacancies separated by $3^{1/2}/2a$ along <111>. Both microdomain types contain a calcium ion on (000) next to the vacancy. This model was used by Proffen, Neder & Frey (1993) analysing the diffuse scattering of a CSZ sample doped with 7 mol% CaO. The proposed model is still under debate in the literature (see references in Neder, Frey & Schulz, 1990*b*; Proffen, Neder & Frey, 1993), particularly the question which cation is the next neighbour of an oxygen vacancy. Dwivedi & Cormack (1990) suggest the calcium ion to be the next-nearest neighbour of the vacancy based on energy calculations. Welberry, Butler, Thompson & Withers (1993), however, attacked the single-vacancy microdomain as being not chemically plausible. Therefore, we reinvestigated this problem by neutron and X-ray data, since Neder, Frey & Schulz (1990*b*) could not fully exclude the existence of microdomains with only zirconium as next neighbours to the oxygen vacancy from their calculations based on neutron scattering data exclusively. The combined refinement of neutron and X-ray data should give a more reliable insight into the defect structure of stabilized zirconia.

## 2. Experimental and measurements

The zirconia samples with the composition $Zr_{0.85}Ca_{0.15}O_{1.85}$ used for neutron and X-ray measurements were grown by the skull melting method and were taken from the same charge delivered by Djevahirdjan S.A., Monthey, Switzerland. The neutron diffraction data used in this study were collected on the neutron spectrometer MAN II at the FRM research reactor in Garching, Munich, Germany, by Neder, Frey & Schulz (1990*b*), *i.e.* the zeroth and second layer of the $[1\bar{1}0]$-zone measured in the integral mode of the spectrometer at wavelength 1.093 Å. The layers were scanned in steps of 0.05 reciprocal lattice constants in the <110> and <001> directions. The X-ray diffraction experiments were carried out on a CAD-4 diffractometer using a graphite monochromator and Mo $K\alpha$ radiation (wavelength 0.7093 Å). The size of the crystal for the X-ray diffraction experiments was *ca* 200 × 100 × 100 $\mu$m. The routine *DIFFUSE* developed by Neder (1994) for the CAD-4 control-software (*EXPRESS*5.1) was used to measure large areas of the reciprocal space. In the X-ray case the zeroth, second and fourth (Figs. 1–3) layers of the $[1\bar{1}0]$-zone were scanned in steps of 0.05 reciprocal lattice constants in the <110> and <001> directions. The measuring time was 20 s for each point.

Two types of diffuse scattering can be observed, broad diffuse bands and diffuse maxima, which can be indexed as satellites with vectors $\pm(0.4,0.4,\pm0.8)$.

* The terms 'domain' and 'microdomain' are used in this paper, because it is common terminology in this context. We are well aware it does not match the strict crystallographic definition of a domain.

The diffuse maxima show remarkable asymmetry. The FWHM of the these diffuse peaks is *ca* 0.25 reciprocal lattice constants corresponding to the correlation length 25 Å. Qualitatively there are no differences between the neutron and X-ray measurements. Quantitatively, however, there are remarkable intensity variations due to the different scattering power of the elements in both cases.

### 3. Model and refinements

The theory of diffraction by correlated microdomains used in this paper was presented by Neder, Frey & Schulz (1990*a*) and Neder & Proffen (1995). The model presented therein consists of two types of microdomains (MD). One type is a microdomain based on a single oxygen vacancy whose next neighbours are relaxed (Fig. 4): Two oxygens, O(1) and O(2), are shifted towards the vacancy along <100> and the four neighbouring cations are relaxed away from the vacancy along <111>. The neighbouring oxygens of the cation $M$ are relaxed away from $M$ in the <111> [O(3)] and <110> [O(4)] directions. As mentioned above, a calcium ion was assumed on (000) for the sake of charge neutrality ($M$ in Fig. 4). Here we also test microdomains containing a zirconium on position $M$. The second microdomain consists of two oxygen vacancies separated by $3^{1/2}/2a$ along <111> with a cation in between (Fig. 5). Again the position marked $M$ in Fig. 5 is now occupied by zirconium or calcium in the different models. The oxygens surrounding the vacancy are relaxed along <100> towards the vacancy and the cations are relaxed along <111> away from the vacancy.

The direction of the vector from the cation $M$ to the oxygen vacancy is taken as the orientation of the microdomain. Eight different orientations result for the 'single-vacancy' microdomain and four for the centrosymmetric 'double-vacancy' microdomain. The theory of Neder, Frey & Schulz (1990*a*) allows to restrict possible orientations of the first neighbour microdomain with respect to a given microdomain. The correlation scheme used in this work is identical to that published by Neder, Frey & Schulz (1990*b*). It restricts the possible orientations for two neighbouring single-vacancy microdomains to parallel $M$-vacancy vectors and those which have an angle of 70.5°. Thus, for a given single-vacancy microdomain of orientation [111], the orientation of the first neighbouring microdomain can be: [111], [$\bar{1}$11], [1$\bar{1}$1] and [11$\bar{1}$]. A double-vacancy microdomain can only be the first neighbour to a single-vacancy domain if its orientation is parallel. The size of

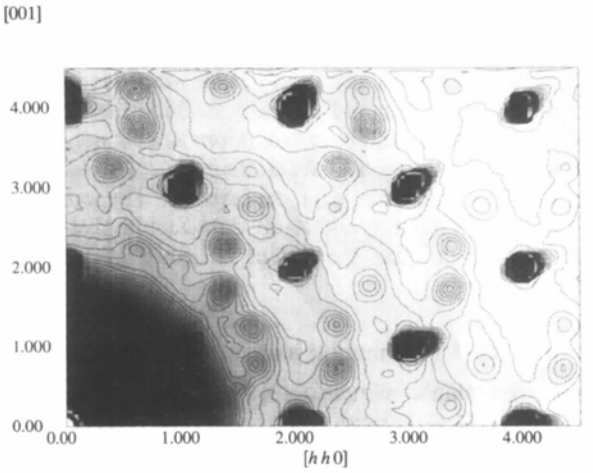


Fig. 1. Zeroth layer of the [1$\bar{1}$0]-zone (X-ray scattering). The intensities are given in steps of 100 counts; the lowest intensity level corresponds to 500 counts.

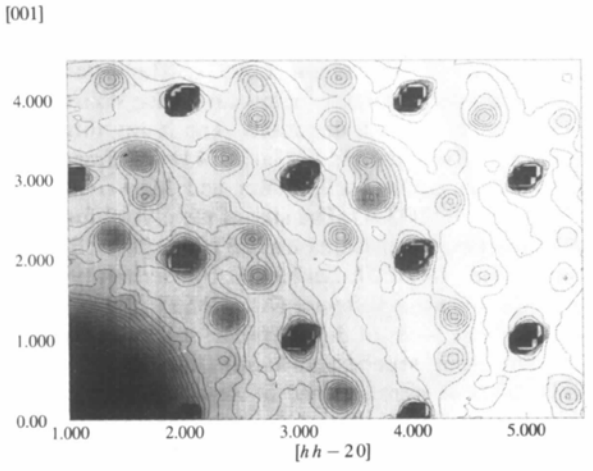


Fig. 2. Second layer of the [1$\bar{1}$0]-zone (X-ray scattering). The intensities are given in steps of 100 counts; the lowest intensity level corresponds to 500 counts.

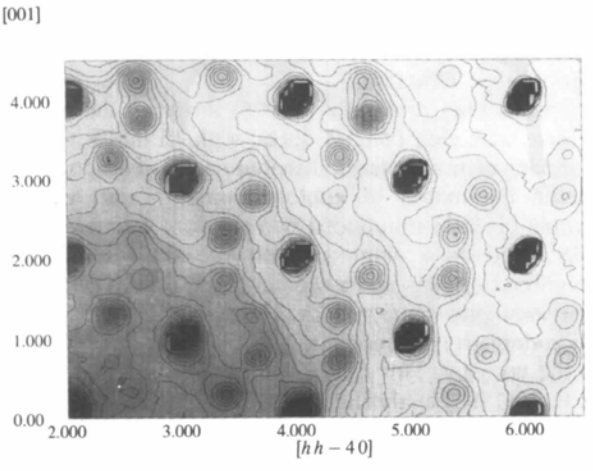


Fig. 3. Fourth layer of the [1$\bar{1}$0]-zone (X-ray scattering). The intensities are given in steps of 100 counts; the lowest intensity level corresponds to 500 counts.

the double-vacancy microdomains is too large compared with the observed modulation wavevector to allow any correlations between two double-vacancy microdomains.

All refinements were carried out with the software package *DOMFIT* (Proffen, Neder & Frey, 1993) modified for simultaneous refinements of neutron and X-ray data. The model parameters were fitted to the observed neutron and X-ray intensities by least-squares and a weighted residual $R$ value was calculated. The peak intensities at the positions in reciprocal space corresponding to the satellite vectors $\pm(0.4,0.4,\pm0.8)$ were used as a data set for the fit. This resulted in a data set of 86 points for the neutron data. In contrast to the flat background of the neutron measurements, the X-ray data show a variable background over the measured reciprocal planes. Since the software can only handle a flat background, the individual background of each diffuse maximum was subtracted before the refinement. The determination of the background was carried out in a window of $0.5 \times 0.5$ reciprocal lattice constants around each diffuse peak. Diffuse peaks with a non-flat background within the window were excluded. The resulting X-ray data set contains 126 points. The following values were kept fixed in all refinements: neutron wavelength 1.093 Å, X-ray wavelength 0.7093 Å (Mo$K\alpha$), Debye–Waller factors, O: 1.00, Zr: 0.50, Ca: 0.50 (Marxreiter, 1988), discrete spacing of the microdomains [$R_0$ in equations (15) and (24) in Neder, Frey & Schulz (1990*a*)] $(1\backslash2)d_{110}$, *i.e.* 3.6 Å, relative abundance of Ca according to 15 mol% CaO and the ratio of single- (66%) and double-vacancy microdomains (33%). Free parameters were: individual overall scale factors for the neutron and X-ray data, one background parameter for neutron data (X-ray background was corrected before the refinements) and all relaxational parameters for the microdomains discussed above (see also Figs. 4 and 5).

## 4. Results

Five models were tested. The only difference between these models is the occupation of the position marked with $M$ in the two microdomain types. Model 1 is exactly the model used by Neder, Frey & Schulz (1990*b*). For all models a simultaneous refinement of neutron and X-ray data was performed. The resulting weighted $R$ value of the combined refinement ('both') and individual weighted $R$ values for the neutron ('n') and X-ray ('X-ray') cases are shown in the right three columns of Table 1. As a second step separate refinements of neutron and X-ray data were carried out using the results of the combined refinement as starting values for the parameters. The corresponding weighted $R$ values are shown in the columns '$R_{wp}$ X-ray' and '$R_{wp}$ n' in Table 1. The expected $R$ values for the combined refinement, neutron and X-ray cases were 3.0, 5.9 and 2.6%, respectively. The results of the simultaneous refinement (Table 1) show that models 1 and 4 with calcium on

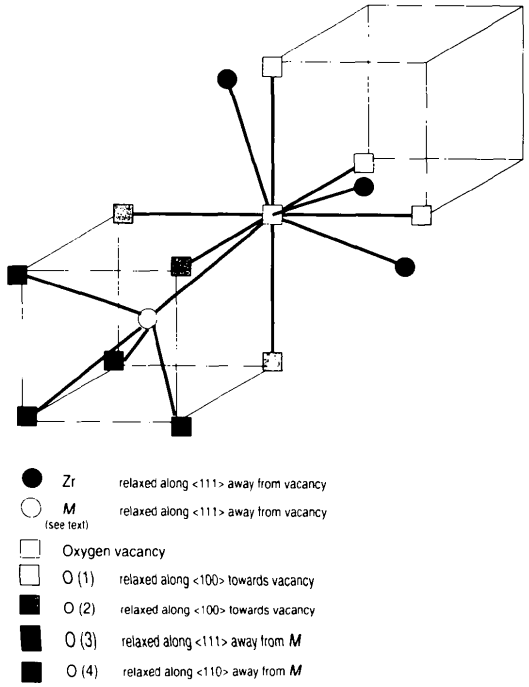


Fig. 4. Structure of a single-vacancy microdomain. The position marked $M$ was occupied by zirconium as well as calcium in the different models. The nearest neighbour ions are relaxed from their positions in the ideal fluorite structure.

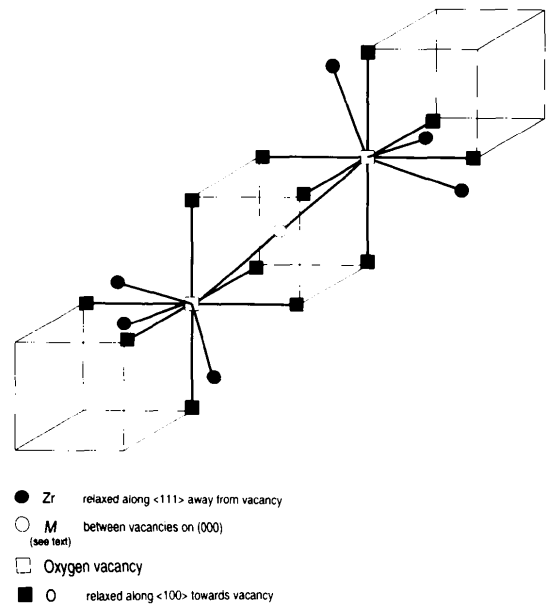


Fig. 5. Structure of a double-vacancy microdomain. The vacancies are separated by $3^{1/2}/2a$ along <111> with a cation ($M$) in between. The position marked $M$ was occupied by zirconium as well as calcium in the different models. The nearest neighbour ions are relaxed from their positions in the ideal fluorite structure.

position $M$ of the single-vacancy microdomain have a significantly higher $R$ value than those models with zirconium on position $M$ and therefore these results support a model with a single-vacancy microdomain only with zirconium as the next neighbour of the oxygen vacancy. Different occupations of the position $M$ in the double-vacancy microdomain lead only to small changes in the resulting weighted $R$ value. Even the combination of neutron and X-ray scattering experiments does not allow to distinguish whether a zirconium or a calcium is located between the oxygen vacancies in the double-vacancy microdomain. There is a small preference for model 3, because the weighted $R$ value is slightly lower and calcium occupies a sixfold coordinated site in the double-vacancy microdomain, as in some other compounds (CaO, $CaCO_3$). The resulting relaxation parameters of the combined refinement of neutron and X-ray data as well as for the separated calculations for model 3 are listed in Table 2. Figs. 6 and 7 show the calculated and difference intensities for the neutron and X-ray cases. All layers show good agreement between observed and calculated data. The most significant result of these refinements is the modified structure of the single-vacancy microdomain with zirconium as the next neighbour of the oxygen vacancy. Even so, some small differences between observed and calculated intensities still remain, which can be classified into three groups: differences in the shape, position and intensity of the diffuse maxima. The different profiles of the observed and calculated diffuse maxima are due to the fixed symmetric distribution function in the present version of the program *DOMFIT*. The parameters for this function were determined by several calculations by Neder, Frey & Schulz (1990*b*). The used data sets

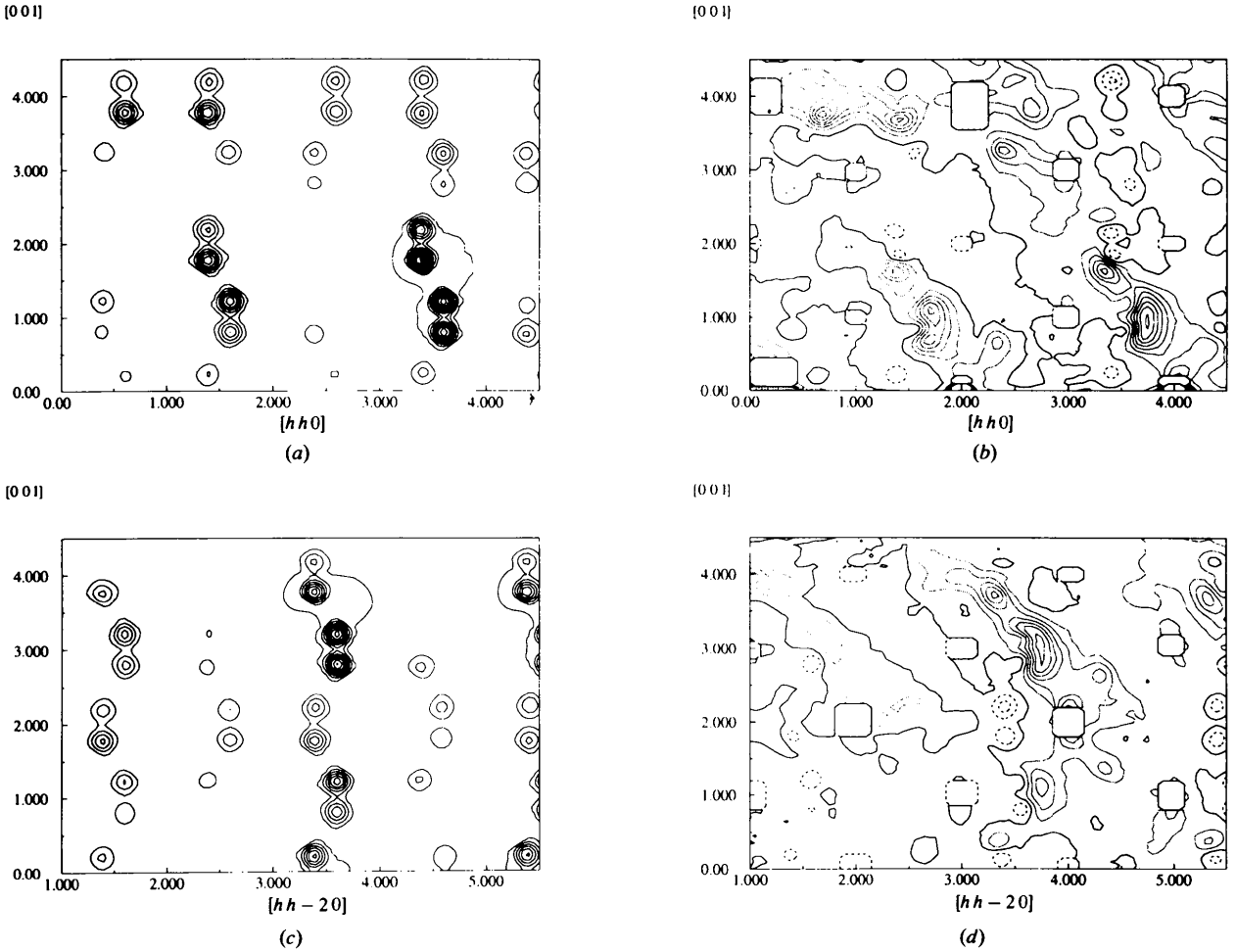


Fig. 6. Left column: Calculated neutron intensity for model 3 in (*a*) the zero and (*c*) the second layer of the [1$\bar{1}$0]-zone. The intensities are given in steps of 50 counts starting at 100 counts. Right column: Difference neutron intensity $I_{obs} - I_{calc}$ for model 3 in (*b*) the zero and (*d*) the second layer of the [110]-zone. The intensities are given in steps of 50 counts. Dotted and dashed lines represent positive and negative values, respectively; the zero level is marked by the solid line.

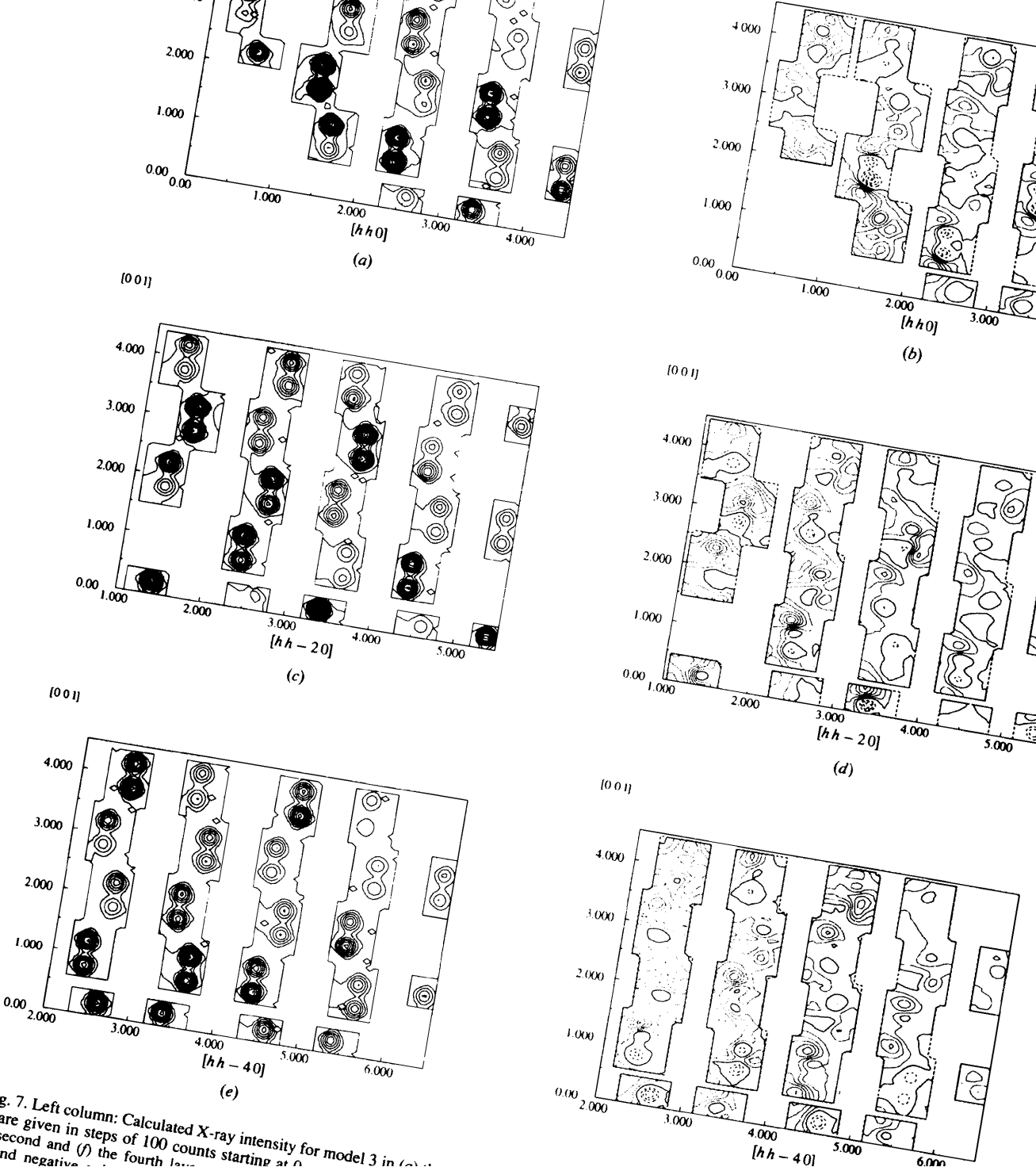


Fig. 7. Left column: Calculated X-ray intensity for model 3 in (a) t
are given in steps of 100 counts starting at 0
second and (f) the fourth lay
and negative

Table 1. *Results of different microdomain models*

The table lists weighted $R$ values for various refinements with different cations on (000) (position marked with $M$) as the next neighbour of the oxygen vacancies in both microdomain types.

| No. | $M$ in single-vacancy MD | $M$ in double-vacancy MD | $R_{wp}$ X-ray (%) | $R_{wp}$ n (%) | $R_{wp}$ (simultaneous refinement) X-ray (%) | n (%) | Both (%) |
|---|---|---|---|---|---|---|---|
| 1 | Ca | Ca | 22.3 | 26.1 | 22.7 | 46.8 | 26.1 |
| 2 | Zr | Zr | 16.2 | 25.1 | 16.1 | 34.8 | 18.8 |
| 3 | Zr | Ca | 15.3 | 24.5 | 15.4 | 35.6 | 18.4 |
| 4 | Ca | Zr | 21.8 | 25.8 | 22.1 | 43.2 | 25.0 |
| 5 | Zr | $Ca_{0.15}Zr_{0.85}$ | 15.9 | 24.7 | 16.0 | 35.0 | 18.7 |

Table 2. *Model* 3: *Relaxations from ideal fluorite positions within the microdomains*

| Ion in MD | Direction of relaxation | Combined n–X-ray | Neutron | X-ray | Neder, Frey & Schulz (1990*b*) |
|---|---|---|---|---|---|
| | | Double-vacancy microdomain relaxation (Å) | | | |
| O | Along ⟨100⟩ | 0.15 (4) | 0.39 (4) | 0.17 (5) | 0.41 (4) |
| Zr | Along ⟨111⟩ | 0.16 (2) | 0.19 (5) | 0.15 (2) | 0.12 (6) |
| | | Single-vacancy microdomain relaxation (Å) | | | |
| O(1) | Along ⟨100⟩ | −0.03 (2) | −0.07 (2) | −0.04 (3) | −0.06 (3) |
| O(2) | Along ⟨100⟩ | 0.19 (3) | 0.20 (3) | 0.20 (4) | 0.16 (3) |
| O(3) | Along ⟨111⟩ | 0.10 (3) | 0.12 (2) | 0.05 (4) | 0.12 (2) |
| O(4) | Along ⟨110⟩ | 0.08 (2) | 0.09 (1) | 0.04 (3) | 0.10 (2) |
| Zr | Along ⟨111⟩ | 0.001 (3) | 0.11 (2) | −0.001 (4) | 0.13 (2) |
| Zr (on M) | Along ⟨111⟩ | 0.21 (1) | 0.31 (4) | 0.21 (2) | 0.30 (5) |

contain only intensities at positions corresponding to the observed satellite vectors, the positions and profiles were not included in the refinements. The fixed modulation wavevector of $\pm(0.4,0.4,\pm0.8)$ resulted in small differences between the calculated and observed position of the diffuse maxima. This can be seen (Figs. 6 and 7) in the differences close to the diffuse maxima. The remaining small differences of the diffuse intensities are due to the model itself. Comparing the results of the separate neutron and X-ray refinements we have equal values within $2\sigma$, except for the parameter 'O' in the double-vacancy microdomain. We have no explanation for this discrepancy. Further calculations with larger microdomains which may contain calcium as a next-next-nearest neighbour can lead to a better description of the defect structure of zirconia.

## 5. Discussion

The simultaneous refinements of neutron and X-ray diffuse scattering data provide a better insight into the defect structure of calcium-stabilized zirconia, because the relative scattering power of Zr compared with O is enhanced in the X-ray case and *vice versa* in the neutron case. The refinements in the frame of a theory of correlated microdomains confirm the essential elements of the defect structure of CSZ presented by Neder, Frey & Schulz (1990*a*,*b*). The defect structure is characterized by two different types of microdomains that are coherently intergrown in the matrix of the cubic crystal. The first microdomain is based on a single oxygen vacancy with relaxed next-nearest neighbours. In contradiction to the earlier results, which are exclusively based on neutron data (Neder, Frey & Schulz, 1990*b*; Proffen, Neder, Frey & Assmus, 1993), the oxygen vacancy is only surrounded by zirconium ions. The second microdomain is based on two vacancies separated by $3^{1/2}/2a$ along ⟨111⟩ with a calcium in between. A final decision as to which cation occupies the site between the vacancies cannot be reached from the present work. The values of the relaxations of the nearest neighbouring ions are identical to those given by Neder, Frey & Schulz (1990*b*) and Proffen, Neder, Frey & Assmus (1993) within the limits of $2\sigma$, except for one parameter which gives somewhat different values for neutron and X-ray refinements.

In a recent study on the influence of an additional applied electric field at high temperatures on the diffuse scattering of zirconia, Kahlert, Frey, Boysen & Lassak (1995) also suggest microdomains where the oxygen vacancies are only connected to Zr. Welberry, Butler, Thompson & Withers (1993) perform Monte Carlo simulations based on measurements of zirconia doped with 19.5 mol% $Y_2O_3$ (YSZ). These authors propose an ordering scheme of the O vacancies in 'zigzag' chains along ⟨111⟩ over oxygen cubes containing a cation site. This basic structural element of oxygen vacancies separated by $3^{1/2}/2a$ along ⟨111⟩ over a cube containing a cation corresponds to the double-vacancy microdomain of this study. From the observed satellite vector of CSZ we cannot deduce any correlations between the double-vacancy microdomains.

One should keep in mind, however, that YSZ and CSZ differ in remarkable details even from a simple chemical point of view ($Ca^{2+}$–$Y^{3+}$).

This work was supported by funds of the BMFT under 05 5WMIAB 7.

### References

Dwivedi, A. & Cormack, A. N. (1990). *Philos. Mag. A*, **61**, 1–22.
Ho, S. M. (1982). *Mater. Sci. Eng.* **54**, 23–29.
Kahlert, H., Frey, F., Boysen, H. & Lassak, K. (1995). *J. Appl. Cryst.* **28**, 812–819.
Marxreiter, J. (1988). Personal communication.
Neder, R. B. (1994). *J. Appl. Cryst.* **27**, 845–846.
Neder, R. B. & Proffen, Th. (1995). In preparation.
Neder, R. B., Frey, F. & Schulz, H. (1990*a*). *Acta Cryst.* A**46**, 792–798.
Neder, R. B., Frey, F. & Schulz, H. (1990*b*). *Acta Cryst.* A**46**, 799–809.
Proffen, Th., Neder, R. B. & Frey, F. (1993). *Z. Kristallogr.* Suppl. 7, 156.
Proffen, Th., Neder, R. B., Frey, F. & Assmus, W. (1993). *Acta Cryst.* B**49**, 599–604.
Rauh, E. G. & Garg, S. P. (1980). *J. Am. Ceram. Soc.* **63**, 239–240.
Subbarao, E. C. (1981), in *Advances in Ceramics*, edited by A. H. Heuer & L. W. Hobbs, Vol. 3, pp. 1–24. Columbus: American Ceramics Society.
Welberry, T. R., Butler, B. D., Thompson, J. G. & Withers, R. L. (1993). *J. Solid State Chem.* **106**, 461–475.